Article
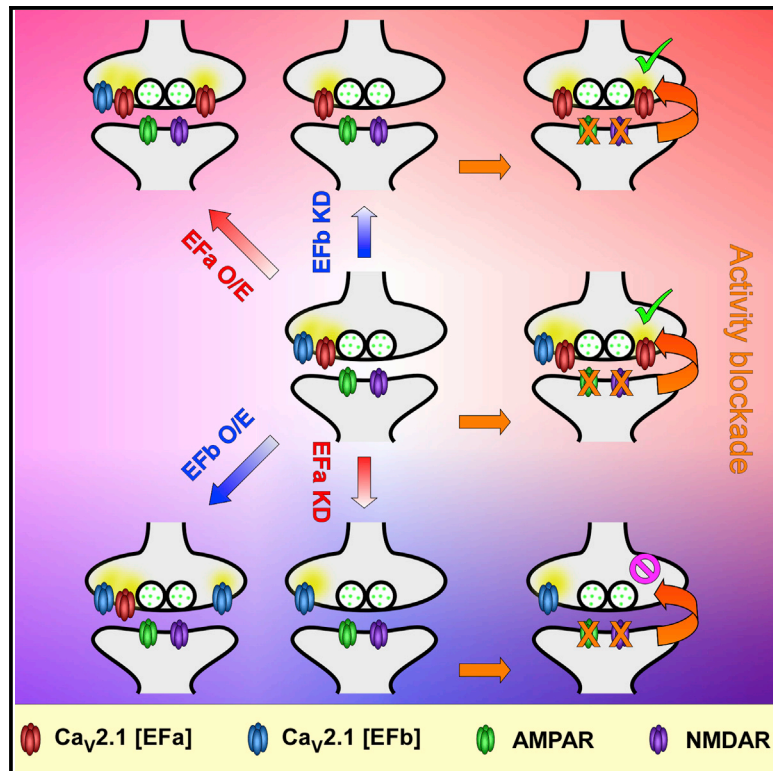
# Alternative Splicing of P/Q-Type Ca$^{2+}$ Channels Shapes Presynaptic Plasticity

## Graphical Abstract



## Authors

Agnes Thalhammer, Andrea Contestabile, Yaroslav S. Ermolyuk, ..., Tuck Wah Soong, Yukiko Goda, Lorenzo A. Cingolani

## Correspondence

lorenzo.cingolani@iit.it

## In Brief

Alternative splicing of Ca$^{2+}$ channels has been hypothesized to contribute to functional diversity in the brain. Thalhammer et al. find that two splice isoforms of P/Q-type Ca$^{2+}$ channels differentially regulate presynaptic plasticity. These results provide evidence that the balance between Ca$^{2+}$ channel isoforms controls synaptic efficacy.

## Highlights

- P/Q-type Ca$^{2+}$ channel splice isoforms couple differentially to transmitter release

- The balance between P/Q-type Ca$^{2+}$ channel isoforms contributes to synaptic efficacy

- Splicing of P/Q-type Ca$^{2+}$ channels regulates short-term synaptic plasticity

- Neurons control P/Q-type Ca$^{2+}$ channel isoform levels in a homeostatic fashion

CellPress

# Article

# Alternative Splicing of P/Q-Type Ca²⁺ Channels Shapes Presynaptic Plasticity

Agnes Thalhammer,[1] Andrea Contestabile,[2] Yaroslav S. Ermolyuk,[3] Teclise Ng,[4,5] Kirill E. Volynski,[3] Tuck Wah Soong,[4,5] Yukiko Goda,[6] and Lorenzo A. Cingolani[1,7,*]

[1]Center for Synaptic Neuroscience and Technology, Istituto Italiano di Tecnologia, Genova 16132, Italy
[2]Department of Neuroscience and Brain Technologies, Istituto Italiano di Tecnologia, Genova 16163, Italy
[3]UCL Institute of Neurology, UCL, London WC1N 3BG, UK
[4]Department of Physiology, Yong Loo Lin School of Medicine, National University of Singapore, Singapore 117456, Singapore
[5]National Neuroscience Institute, 11 Jalan Tan Tock Seng, Singapore 308433, Singapore
[6]RIKEN Brain Science Institute, Wako, Saitama 351-0198, Japan
[7]Lead Contact
*Correspondence: lorenzo.cingolani@iit.it
http://dx.doi.org/10.1016/j.celrep.2017.06.055

## SUMMARY

**Alternative splicing of pre-mRNAs is prominent in the mammalian brain, where it is thought to expand proteome diversity. For example, alternative splicing of voltage-gated Ca²⁺ channel (VGCC) α₁ subunits can generate thousands of isoforms with differential properties and expression patterns. However, the impact of this molecular diversity on brain function, particularly on synaptic transmission, which crucially depends on VGCCs, is unclear. Here, we investigate how two major splice isoforms of P/Q-type VGCCs (Ca_v2.1[EFa/b]) regulate presynaptic plasticity in hippocampal neurons. We find that the efficacy of P/Q-type VGCC isoforms in supporting synaptic transmission is markedly different, with Ca_v2.1[EFa] promoting synaptic depression and Ca_v2.1[EFb] synaptic facilitation. Following a reduction in network activity, hippocampal neurons upregulate selectively Ca_v2.1[EFa], the isoform exhibiting the higher synaptic efficacy, thus effectively supporting presynaptic homeostatic plasticity. Therefore, the balance between VGCC splice variants at the synapse is a key factor in controlling neurotransmitter release and presynaptic plasticity.**

## INTRODUCTION

The majority of neuronal genes are subject to alternative splicing, which is thought to increase proteome complexity and optimize protein function to specific cellular tasks (Lipscombe et al., 2013; Raj and Blencowe, 2015). In support of a dedicated function of individual splice variants, some mutations that cause brain diseases impair only one of the splice isoforms of a neuronal gene (Simms and Zamponi, 2014) (Figure 1B). Yet there are few studies investigating how alternative splicing regulates physiological events in neurons.

Here, we examine how alternatively spliced variants of Ca_v2.1 (P/Q-type) channels, which are the predominant voltage-gated Ca²⁺ channels (VGCCs) at most fast synapses in the CNS, regulate synaptic transmission. Alternative splicing of the pore-forming α₁ subunit of Ca_v2.1 (α_1A) can potentially generate thousands of splice isoforms displaying differential expression patterns and divergent biophysical properties (Soong et al., 2002). Among them, alternative splicing of the mutually exclusive exons 37a and 37b produces two major variants, Ca_v2.1[EFa] and Ca_v2.1 [EFb], which diverge in an EF-hand-like domain located in the proximal C terminus of the channel (Figures 1A and 1B) (Bourinet et al., 1999; Chaudhuri et al., 2004; Soong et al., 2002). Whereas Ca_v2.1[EFb] predominates at early stages of development, both splice isoforms are expressed in comparable amounts in most regions of the adult brain, as for example in the hippocampus (Bourinet et al., 1999; Chaudhuri et al., 2004; Soong et al., 2002; Vigues et al., 2002).

Their biophysical properties, studied in non-neuronal cells to date, differ as well: Ca_v2.1[EFa] generates slowly activating currents, whose kinetics are accelerated by Ca²⁺ influx through the channel during a preceding pulse (Ca²⁺-dependent facilitation), whereas Ca_v2.1[EFb] produces currents that are faster than those of Ca_v2.1[EFa] under basal conditions and are not further facilitated by Ca²⁺ (Chaudhuri et al., 2004).

Despite prominent expression in the brain and divergent functional properties, it is not known whether these two splice isoforms, or any other Ca_v2.1 splice variant, are specialized to fulfill specific cellular tasks in neurons. Here, we have focused on Ca_v2.1[EFa] and Ca_v2.1[EFb] and asked whether and how they differentially regulate synaptic transmission and plasticity in hippocampal pyramidal neurons.

By manipulating bi-directionally the relative abundance of Ca_v2.1[EFa] and Ca_v2.1[EFb] isoforms, we reveal that they regulate neurotransmitter release and short-term synaptic plasticity in opposite directions: Ca_v2.1[EFa] boosts synaptic efficacy and promotes synaptic depression, while Ca_v2.1[EFb] tilts the balance toward low synaptic efficacy and synaptic facilitation. Importantly, neuronal activity regulates the relative abundance of the two Ca_v2.1 splice isoforms in a homeostatic fashion. In response to a reduction in network excitability, hippocampal
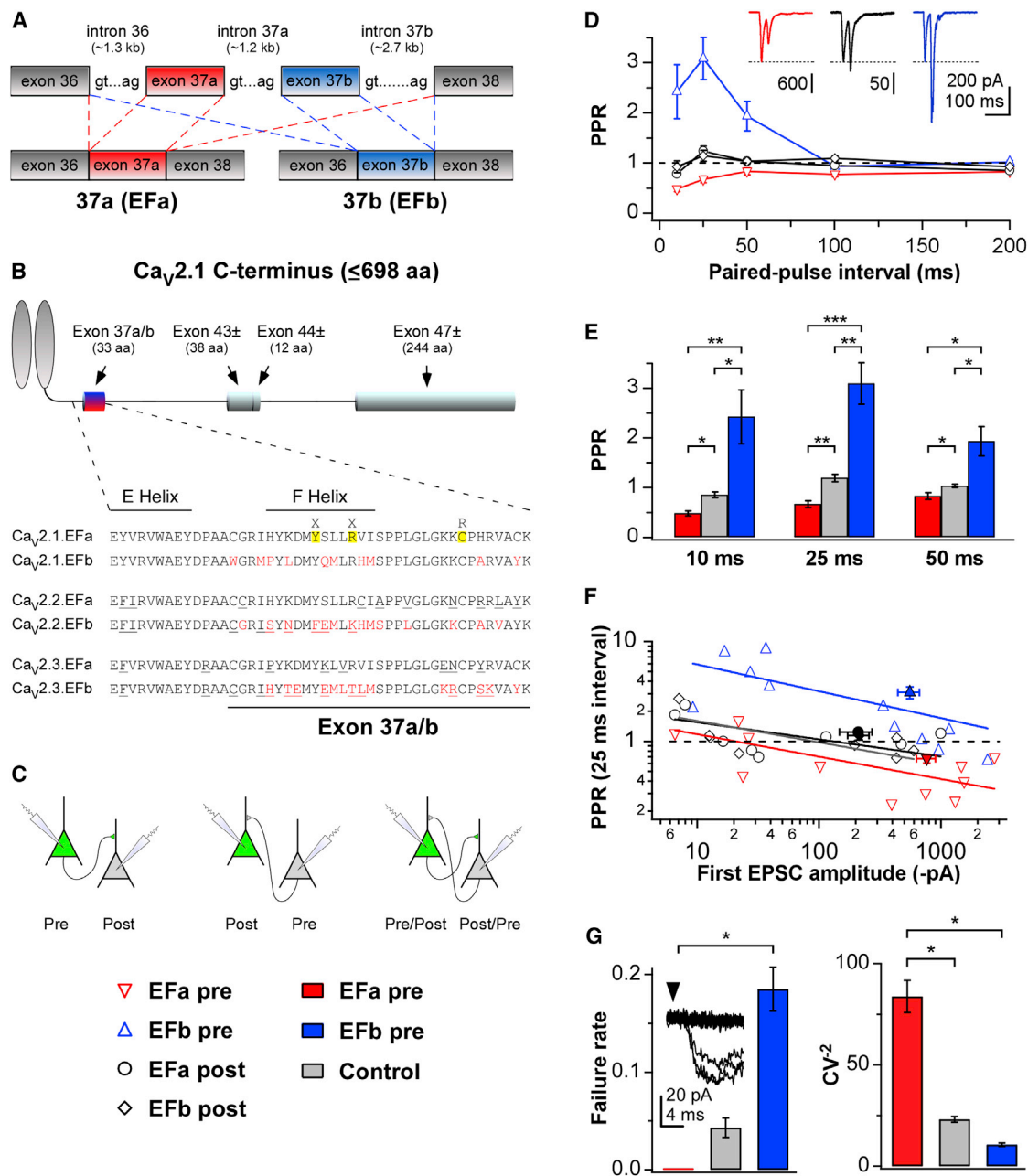
**Figure 1. Presynaptically Expressed $Ca_v2.1[EFa]$ and $Ca_v2.1[EFb]$ Differentially Regulate Short-Term Synaptic Plasticity**

(A) Postulated mechanism of alternative splicing for exon 37a/b. Either exon 37a or 37b is included in the final mRNA, resulting in two mutually exclusive splice isoforms of an EF-hand-like domain (EFa and EFb). Scheme adapted from Soong et al. (2002).

(B) Top: cartoon of the cytoplasmic C terminus of the human $Ca_v2.1$ $α_1$ subunit drawn to scale. Exons 37a/b (red/blue) are depicted in relationship to the other alternative exons. Bottom: alternative splicing of exons 37a/b is conserved within $Ca_v2$ channels. Differences between splice isoforms are indicated in red, and those between $Ca_v2.1$, $Ca_v2.2$, and $Ca_v2.3$ are underscored. Residues highlighted in yellow have been found mutated in patients with episodic ataxia type 2 (Graves et al., 2008; Mantuano et al., 2010).

(C) Recording configurations in primary hippocampal cultures for experiments as in (D–G). Green indicates transfected neurons.

(D) Paired-pulse ratios (PPRs) versus paired-pulse intervals for paired recordings between hippocampal pyramidal neurons. Presynaptic expression of $Ca_v2.1$ [EFa] favors paired-pulse depression (PPD; EFa pre, red, n = 11 recordings), while presynaptic expression of $Ca_v2.1[EFb]$ induces strong paired-pulse facilitation (PPF; EFb pre, blue, n = 11 recordings); a PPR close to 1 is observed when either $Ca_v2.1[EFa]$ or $Ca_v2.1[EFb]$ is expressed postsynaptically (EFa post and EFb post, black, n = 8 recordings each). Inset: representative EPSCs for the 25 ms paired-pulse interval. Traces are averages of three trials (red, EFa pre; black, EFa post; blue, EFb pre).

(E) Summary of PPRs at 10, 25, and 50 ms paired-pulse intervals, showing PPD for EFa pre and PPF for EFb pre. Because no differences were detected between EFa post and EFb post in (D), the two groups were pooled (control; *p < 0.04, **p ≤ 0.01, and ***p < 0.0001).

*(legend continued on next page)*

neurons upregulate selectively $Ca_v2.1$[EFa], the splice isoform displaying the higher synaptic efficacy, thus effectively counteracting the decrease in network activity.

## RESULTS

### $Ca_v2.1$ Splice Variants Are Targeted to Presynaptic Boutons Where They Differentially Regulate $P_r$ and Short-Term Synaptic Plasticity

In order to compare the relative contributions of $Ca_v2.1$[EFa] and $Ca_v2.1$[EFb] splice isoforms to synaptic transmission, we first took an overexpression approach. Confocal imaging showed that both isoforms were efficiently targeted to axons and presynaptic boutons in primary hippocampal neurons (Figure S1), where they partially replaced endogenous $Ca_v2.1$ channels (Figure S2). The level of co-localization with the presynaptic cytomatrix protein bassoon was overall higher for $Ca_v2.1$[EFa] than for $Ca_v2.1$[EFb] (Figure S1D). We next asked whether the exogenously expressed $Ca_v2.1$ splice variants affected presynaptic $Ca^{2+}$ transients. First, we used a presynaptically localized $Ca^{2+}$ indicator, SyGCaMP3, in which GCaMP3 was fused to synaptophysin (Dreosti et al., 2009), to qualitatively monitor changes in presynaptic $Ca^{2+}$ levels (see Supplemental Experimental Procedures). Expression of either splice isoform strongly increased presynaptic $Ca^{2+}$ signals, with $Ca_v2.1$[EFa] inducing larger transients than $Ca_v2.1$[EFb] (Figures S3A–S3C). To quantitatively compare presynaptic $Ca^{2+}$ signals between the two isoforms, we used Fluo-4, a $Ca^{2+}$ indicator providing a linear readout of action potential (AP)-evoked presynaptic $Ca^{2+}$ influx (see Supplemental Experimental Procedures). In response to two successively applied APs, $Ca_v2.1$[EFb] induced a small ($\sim$10%) but significantly higher facilitation of presynaptic $Ca^{2+}$ transients relative to $Ca_v2.1$[EFa] (Figures S3D–S3G). If we consider that there is a steep power dependence of release probability ($P_r$) on $Ca^{2+}$ entry, the observed differences in presynaptic $Ca^{2+}$ transients between $Ca_v2.1$[EFa] and $Ca_v2.1$[EFb] could also produce differences in the efficacy of neurotransmitter release and short-term synaptic plasticity.

In order to determine whether the two splice isoforms differentially regulated synaptic efficacy and plasticity, we performed paired recordings from monosynaptically connected primary hippocampal pyramidal neurons with only one of the two neurons transfected with either $Ca_v2.1$[EFa] or $Ca_v2.1$[EFb] (Figure 1C). Strikingly, presynaptic expression of the two splice isoforms affected paired-pulse ratio (PPR) of evoked excitatory

postsynaptic currents (EPSCs) in opposite directions. $Ca_v2.1$[EFa] promoted paired-pulse depression (PPD), with a concomitant decrease in failure rate and an increase in $CV^{-2}$ (coefficient of variation) of EPSC amplitudes (Figures 1D–1G), suggesting an increase in $P_r$ (Chavez-Noriega and Stevens, 1994). In contrast, $Ca_v2.1$[EFb] induced prominent paired-pulse facilitation (PPF), increased failure rate, and decreased $CV^{-2}$ (Figures 1D–1G). Altogether, these changes were consistent with $Ca_v2.1$[EFa] enhancing and $Ca_v2.1$[EFb] reducing $P_r$.

To corroborate the changes in $P_r$ by $Ca_v2.1$ splice isoforms, we next used the NMDA receptor (NMDAR) open channel blocker MK-801, whose rate of block of NMDAR EPSCs is indicative of $P_r$, with higher $P_r$ synapses producing a faster rate of decay (Hessler et al., 1993; Rosenmund et al., 1993). As shown in Figure 2, expression of $Ca_v2.1$[EFa] and $Ca_v2.1$[EFb] differentially affected the progressive block of NMDAR responses by MK-801. Although both splice isoforms accelerated the MK-801-dependent block of synaptic NMDAR EPSCs, $Ca_v2.1$[EFa] was more effective than $Ca_v2.1$[EFb]. In particular, the number of stimuli necessary to achieve a 50% block of NMDAR EPSCs with MK-801 was significantly reduced only by $Ca_v2.1$[EFa] ($3.50 \pm 0.62$, $9.29 \pm 0.72$, and $6.56 \pm 0.80$ stimuli for $Ca_v2.1$[EFa], control, and $Ca_v2.1$[EFb], respectively; Figure 2C), indicating that neurons expressing $Ca_v2.1$[EFa] exhibit overall higher $P_r$ than naive neurons.

Collectively, these findings suggest that $Ca_v2.1$ splice isoforms differentially regulate $P_r$ and short-term synaptic plasticity.

### $Ca_v2.1$ Splice Isoforms Are Differentially Coupled to the Neurotransmitter Release Machinery

Motivated by previous findings in which the efficacy of AP-driven neurotransmitter release is affected by the localization of $Ca^{2+}$ channels at the active zone (AZ; Kaeser et al., 2011; Mochida et al., 1996; Wu et al., 1999), we examined whether the observed differences in synaptic efficacy between $Ca_v2.1$[EFa] and $Ca_v2.1$[EFb] reflected a differential functional coupling of the two isoforms to the neurotransmitter release machinery. If the lower $P_r$ and strong PPF associated with $Ca_v2.1$[EFb] were due to a less efficient coupling of this channel to the release machinery, then the slow $Ca^{2+}$ chelator EGTA should be more effective in intercepting $Ca^{2+}$ and inhibiting exocytosis for $Ca_v2.1$[EFb] than for $Ca_v2.1$[EFa]. We tested this hypothesis with two complementary approaches. First, we used synaptophysin-pHluorin (SypHy) to directly monitor vesicle turnover before and after application of EGTA-AM under conditions that deplete the readily releasable

---

(F) PPR at 25 ms interval versus first EPSC amplitude showing that the differences in PPR between the two splice isoforms are observed across a broad range of EPSC amplitudes; lines are linear regression fits of the log-transformed data (black line, EFa post; gray line, EFb post). Open symbols represent individual recordings, filled symbols population averages.

(G) Left, presynaptic expression of $Ca_v2.1$[EFb] induces a high failure rate of synaptic transmission. Failures were never observed with presynaptic $Ca_v2.1$[EFa] (n = 11 pairs), but they were present in 2 of 16 control recordings, in which the presynaptic neuron was untransfected (failure rate, amplitude without failures of the first synchronous EPSC, and median amplitude of the asynchronous release: 0.63, −7.1 pA, and −8.5 pA [21 events] for the first pair and 0.06, −6.6 pA, −6.5 pA [5 events] for the second pair) and in 5 of 11 recordings with presynaptic $Ca_v2.1$[EFb] (failure rate, amplitude without failures of the first synchronous EPSC, and median amplitude of the asynchronous release: 0.07, −16.7 pA, and −19.4 pA [44 events] for the first pair; 0.07, −38.9 pA, and −21.9 pA [38 events] for the second pair, 0.78, −36.5 pA; −30.1 pA [9 events] for the third pair; 0.67, −27.2 pA, and −28.1 pA [11 events] for the fourth pair; and 0.46, −9.2 pA, and −8.5 pA [8 events] for the fifth pair; *p < 0.05). Inset: 17 consecutive EPSCs for an EFb pre pair, showing high failure rate. Right: summary of the effects of $Ca_v2.1$ splice isoforms on the coefficient of variation (CV) of evoked EPSCs. Presynaptic $Ca_v2.1$[EFa] induces a significant increase in $CV^{-2}$ relative to presynaptic untransfected neurons (control) and presynaptic $Ca_v2.1$[EFb] (*p < 0.05), consistent with an increase in $P_r$.

Data are presented as mean ± SEM. See also Figures S1–S3.

## A
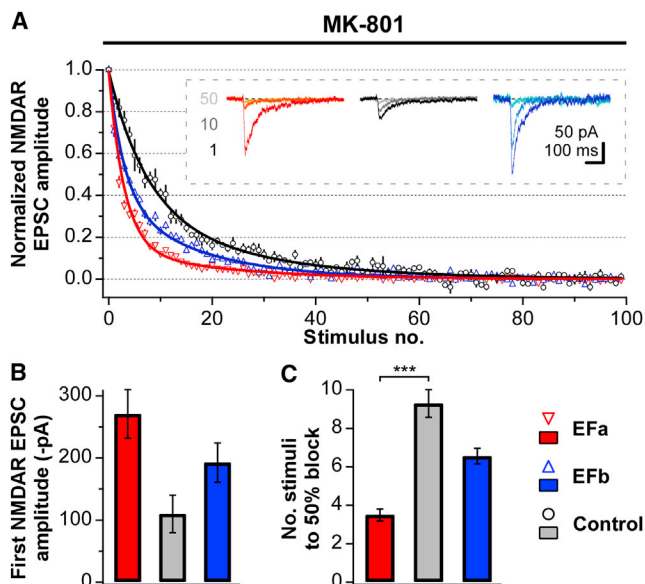


**MK-801**

**Figure 2. Ca$_v$2.1[EFa] and Ca$_v$2.1[EFb] Differentially Regulate P$_r$**

(A) Plot of the effects of the open-channel blocker MK-801 (5 μM) on NMDAR currents in primary hippocampal pyramidal neurons; recording configuration as in Figure 1. The decay rates of NMDAR EPSCs were fit by the sum of two decaying exponentials (f[x] = A$_{fast}$*exp[−x/τ$_{fast}$] + A$_{slow}$ × exp[−x/τ$_{slow}$]). The progressive block of NMDAR responses by MK-801 is accelerated by presynaptic expression of Ca$_v$2.1[EFa] (red, n = 10 recordings) and, to a lesser extent, by that of Ca$_v$2.1[EFb] (blue, n = 9 recordings), compared with control (black, n = 7 recordings). Inset: representative NMDAR EPSCs for the 1st, 10th, and 50th stimulus.

(B) Mean amplitude of first NMDAR EPSCs.

(C) Summary of the number of stimuli necessary to achieve a 50% block of NMDAR EPSCs with MK-801 for experiments as in (A) (***p < 0.001).

Data are presented as mean ± SEM. See also Figures S1–S3.

pool (RRP; 40 APs at 20 Hz). We chose concentrations and incubation times of the chelator that produced ~50% reduction in exocytosis in control neurons (Hoppa et al., 2012). EGTA-AM decreased vesicle release by nearly 70% in boutons expressing Ca$_v$2.1[EFb], whereas it had little effect in the presence of Ca$_v$2.1 [EFa] (Figures 3A and 3B).

Because multiple Ca$^{2+}$-dependent mechanisms are at work in response to trains of APs, we next used electrophysiology to examine the effects of EGTA on EPSCs evoked by individual APs. We found that Ca$_v$2.1[EFa] minimized while Ca$_v$2.1[EFb] enhanced the EGTA-dependent decrease in the amplitude of EPSCs (Figure 3C). EGTA also abolished selectively the PPF observed in the presence of Ca$_v$2.1[EFb] (Figure 3D), suggesting that facilitation was largely driven by accumulation of residual free Ca$^{2+}$ in neurons expressing Ca$_v$2.1[EFb].

Taken together, these findings support a model whereby Ca$_v$2.1[EFa] and Ca$_v$2.1[EFb] are differentially coupled to the neurotransmitter release machinery.

### Endogenous Ca$_v$2.1 Splice Isoforms Control Presynaptic Ca$^{2+}$ Influx and Vesicle Release

Thus far, we have taken an overexpression approach to probe the differential properties of the two Ca$_v$2.1 splice variants. We next

addressed whether the effects of exogenously expressed Ca$_v$2.1[EFa] and Ca$_v$2.1[EFb] reflected the function of the respective endogenous Ca$_v$2.1 isoforms. First, we developed isoform-specific microRNAs (miRs) to knockdown selectively Ca$_v$2.1[EFa] or Ca$_v$2.1[EFb] (Figure S4A and Supplemental Experimental Procedures) and assessed by confocal microscopy (Figures 4A–4F) that silencing either Ca$_v$2.1[EFa] or Ca$_v$2.1[EFb] effectively reduced immunofluorescence signal of total Ca$_v$2.1 in presynaptic boutons (−40 ± 8.1% and −50 ± 7.6% for miR EFa1 and miR EFa3, which both target Ca$_v$2.1[EFa], and −52 ± 7.1% for miR EFb2, which targets Ca$_v$2.1[EFb]; Figures 4A and 4B). Notably, knockdown of Ca$_v$2.1[EFb] resulted in an increase in the extent of co-localization of Ca$_v$2.1 with the presynaptic marker bassoon (Figures 4A and 4D), suggesting that endogenous Ca$_v$2.1[EFa] is more tightly localized with presynaptic scaffold proteins than Ca$_v$2.1[EFb].

To determine whether the reduction in presynaptic expression of Ca$_v$2.1 was accompanied by changes in Ca$^{2+}$ transients, we used the highly sensitive presynaptic Ca$^{2+}$ indicator SyGCaMP6s (see Supplemental Experimental Procedures), because an overall decrease in Ca$^{2+}$ entry was expected. Indeed, knockdown of either Ca$_v$2.1[EFa] or Ca$_v$2.1[EFb] decreased AP-triggered presynaptic Ca$^{2+}$ signals across a broad range of stimulus intensities (Figures S4D–S4F). Moreover, targeting both splice isoforms nearly abolished measurable Ca$^{2+}$ transients in response to one or two APs (Figures S4D and S4F), in further support of the effectiveness of our knockdown approach.

Next, we tested if the differences in the localization of Ca$_v$2.1 splice isoforms (Figures 4A and 4D) were associated with differences in their function at the synapse. As measured by the SypHy assay, knockdown of Ca$_v$2.1[EFa] significantly increased the sensitivity of vesicle turnover to EGTA-AM, (~80% reduction in SypHy responses relative to baseline versus ~50% in controls); in contrast, knockdown of Ca$_v$2.1[EFb] did not increase EGTA sensitivity (Figures 5, S4B, and S4C). These findings therefore suggest that endogenous Ca$_v$2.1[EFb] is the splice variant more sensitive to EGTA in naive conditions.

### Endogenous Ca$_v$2.1 Splice Isoforms Differentially Regulate Short-Term Synaptic Plasticity in Intact Hippocampal Circuits

To investigate whether alternative splicing at the EF-hand-like domain of Ca$_v$2.1 is important for short-term synaptic plasticity in intact brain circuits, we knocked down either Ca$_v$2.1[EFa] or Ca$_v$2.1[EFb] in the hippocampus, where both splice isoforms are expressed at comparable levels (42.9 ± 0.8% and 57.1 ± 0.8% transcript expression levels for Ca$_v$2.1[EFa] and Ca$_v$2.1[EFb], respectively; see Supplemental Experimental Procedures). To monitor synaptic transmission selectively at connections where presynaptic neurons were knocked down for the Ca$_v$2.1 splice variants, we stereotactically injected adeno-associated viruses (AAVs) expressing Ca$_v$2.1 splice isoform-specific miRs along with the ultrafast channelrhodopsin ChETA (Gunaydin et al., 2010) fused to the fluorescent protein TdTomato into area CA3 of the rat hippocampus (Figures 6A, 6B, and S5A and Supplemental Experimental Procedures).

We then prepared acute hippocampal slices from AAV-injected animals and evoked AP-dependent, AMPAR-mediated
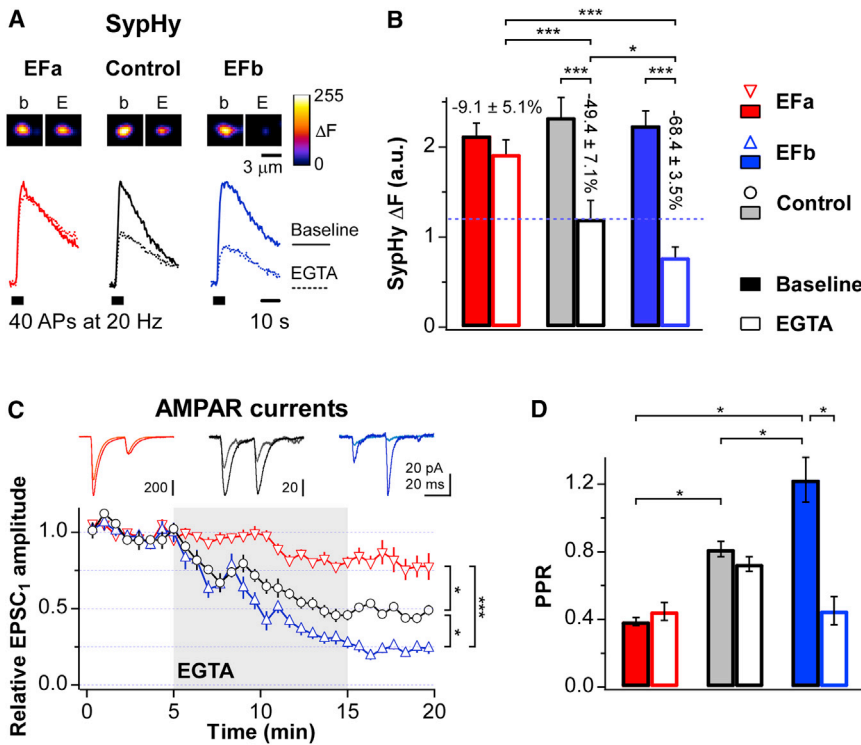
**Figure 3. Ca_v2.1[EFa] and Ca_v2.1[EFb] Are Differentially Coupled to the Neurotransmitter Release Machinery**

(A) SypHy responses for Ca_v2.1[EFa], Ca_v2.1[EFb], and control to 40 APs at 20 Hz before (continuous line) and after (dotted line) EGTA-AM application (200 $\mu$M; loaded for 90 s, followed by 10 min wash). Traces are normalized to pre-EGTA responses in control. Inset: individual boutons for the three conditions (b, pre-EGTA; E, post-EGTA).

(B) Summary of experiments as in (A) showing that sensitivity of vesicle turnover to EGTA is decreased by Ca_v2.1[EFa] and increased by Ca_v2.1[EFb] (n = 9, 9, and 7 independent experiments for Ca_v2.1[EFa], Ca_v2.1[EFb], and control, respectively; *p < 0.05 and ***p < 0.001).

(C) Time course of the effects of EGTA-AM (50 $\mu$M) on the amplitude of the first of two EPSCs evoked in primary hippocampal pyramidal neurons. Recording configuration is as in Figure 1, with a 25 ms paired-pulse interval. Gray area indicates the period of EGTA-AM application. Relative to controls (black, n = 10 recordings), presynaptic expression of Ca_v2.1[EFa] (red, n = 6 recordings) and Ca_v2.1[EFb] (blue, n = 8 recordings) minimizes and accentuates the EGTA-dependent decrease in AMPAR EPSCs, respectively (*p < 0.05 and ***p < 0.001). This is consistent with Ca_v2.1[EFa] and Ca_v2.1[EFb] being tightly and loosely coupled to the release machinery, respectively. Inset: representative EPSC pairs before (darker) and after (lighter traces) EGTA-AM application.

(D) Summary of PPRs under basal conditions (filled bars) and after application of EGTA-AM (open bars) from experiments in (C). Application of EGTA-AM abolishes PPF that accompanies presynaptic expression of Ca_v2.1[EFb], suggesting an involvement of residual free $Ca^{2+}$ in the Ca_v2.1[EFb]-dependent facilitation (*p < 0.05).

Data are presented as mean ± SEM. See also Figures S1–S3.

EPSCs in CA1 pyramidal neurons by stimulating CA3 somata with brief blue light pulses (2 ms long; Figures 6C, S5B, and S5C). We found that knockdown of Ca_v2.1 splice isoforms affected responses to paired-pulse stimulation in opposite directions: knockdown of Ca_v2.1[EFa] boosted PPF, whereas knockdown of Ca_v2.1[EFb] abolished it (Figures 6D, 6E, and S5D).

Synaptic transmission is mediated mostly by P/Q-type and N-type $Ca^{2+}$ channels at these synapses (Reid et al., 1998; Scholz and Miller, 1995). To rule out the possibility that some of the effects we observed upon knockdown of P/Q-type Ca_v2.1 splice isoforms were due to a compensatory upregulation of N-type channels, we repeated the above experiments in the presence of $\omega$-conotoxin GVIA to block N-type channels. As shown in Figures S5E and S5F, the increase in PPR with miRs directed against Ca_v2.1[EFa] and its decrease with miR against Ca_v2.1[EFb] were still observed after blockade of N-type channels. Taken together, these data suggest that Ca_v2.1[EFa] and Ca_v2.1[EFb] splice variants shape short-term plasticity at hippocampal synapses.

**Neurons Regulate the Expression of Ca_v2.1[EFa] in a Homeostatic Fashion**

We next investigated whether hippocampal neurons modulate the balance between the two Ca_v2.1 splice variants to regulate synaptic efficacy in an activity-dependent manner. We turned

to a presynaptic form of homeostatic plasticity whereby neurons scale up presynaptic efficacy to counterbalance a chronic reduction in network excitability. This form of plasticity depends, at least in part, on changes in presynaptic $Ca^{2+}$ and Ca_v2.1 channels (Frank et al., 2006; Jakawich et al., 2010; Zhao et al., 2011).

First, we tested if inducing homeostatic plasticity affected the expression of Ca_v2.1 splice isoforms. As shown in Figure 7A, two different activity deprivation protocols commonly used to induce homeostatic plasticity in primary cultures scaled up the transcript of Ca_v2.1[EFa] but not that of Ca_v2.1[EFb], with the effects peaking at 24 hr. We next determined whether the activity-dependent changes at the mRNA level were reflected in changes in protein content for Ca_v2.1 at the synapse. Chronic activity deprivation scaled up synaptic Ca_v2.1 in control conditions (Figures 7B and 7C), in agreement with previous observations (Lazarevic et al., 2011). Remarkably, this effect was blocked by knockdown of Ca_v2.1[EFa] but not by that of Ca_v2.1[EFb] (Figures 7B and 7C), suggesting that only Ca_v2.1[EFa] expression is regulated by activity and that the synaptic increase in Ca_v2.1 content upon activity deprivation is due mainly to Ca_v2.1[EFa].

To investigate changes in presynaptic function directly, we examined activity-dependent vesicle turnover by monitoring the uptake of an antibody against the luminal domain of synaptotagmin (Stg). In line with previous reports (Jakawich et al., 2010), we found that Stg uptake was dependent on P/Q-type
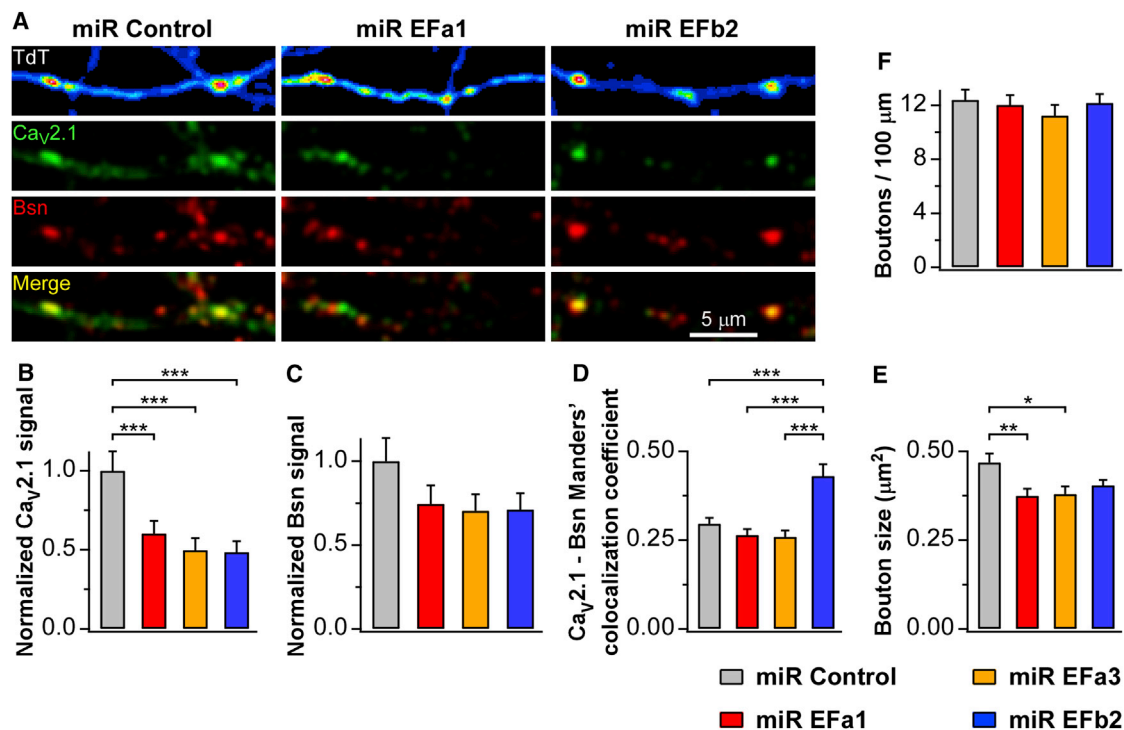
**Figure 4. Splice Isoform-Specific MicroRNAs Reduce Endogenous Ca$_v$2.1 Channels at Presynaptic Boutons**
(A) Confocal microscopy images of primary hippocampal axons expressing TdTomato and the indicated microRNAs (miRs). Bassoon (Bsn) and TdTomato (TdT) were used as presynaptic and morphological markers, respectively. Ca$_v$2.1 was detected with an antibody recognizing both splice isoforms.
(B) Quantification of experiments as in (A) indicating that knockdown of either Ca$_v$2.1[EFa] (miR EFa1, red, or miR EFa3, orange) or Ca$_v$2.1[EFb] (miR EFb2, blue) reduces endogenous Ca$_v$2.1 in axons to a similar extent, relative to the negative control (miR control, gray).
(C) Quantification of the effects of the indicated miRs on bassoon expression.
(D) Mander's co-localization coefficient for Ca$_v$2.1 with bassoon is selectively and largely increased by knockdown of Ca$_v$2.1[EFb], suggesting that endogenous Ca$_v$2.1[EFa] co-localizes with bassoon better than Ca$_v$2.1[EFb].
(E and F) Quantification of the effects of the indicated miRs on bouton size (E) and number (F) (n = 32, 41, 33, and 38 fields of view for miR control, miR EFa1, miR EFa3, and miR EFb2, respectively; *p < 0.05, **p < 0.01, and ***p < 0.001).
Data are presented as mean ± SEM. See also Figure S4.

channels, because ω-agatoxin TK, a blocker of these channels, reduced the uptake under basal (untreated) and activity-deprived conditions (CNQX/DAPV; Figures 7D and 7E). Notably, although knockdown of either splice variant reduced Stg uptake under basal conditions, only knockdown of Ca$_v$2.1[EFa] prevented the increase in Stg uptake that followed activity deprivation (Figures 7B, 7D, and 7E). Altogether, these findings indicate that homeostatic upregulation of presynaptic release induced by activity deprivation is selectively dependent on Ca$_v$2.1[EFa], the splice isoform exhibiting higher synaptic efficacy.

## DISCUSSION

We have combined electrophysiological recordings with optogenetic stimulation, along with imaging of presynaptic Ca$^{2+}$ and vesicle turnover, to assess how two major mutually exclusive splice isoforms of P/Q-type channels (Ca$_v$2.1[EFa] and Ca$_v$2.1[EFb]; Figures 1A and 1B) regulate excitatory synaptic transmission and presynaptic plasticity in hippocampal neurons. In particular, the use of optogenetics to selectively stimulate neurons expressing isoform-specific miRs enabled us to examine the role of alternatively spliced Ca$_v$2.1 variants in intact hippocampal circuits. Such a strategy may be generally applicable for studies of the physiological significance of presynaptically expressed proteins in synaptic transmission.

We propose that P/Q-type Ca$_v$2.1 channels do not constitute a uniform population with respect to their efficacy for eliciting vesicle release. In particular, the two mutually exclusive Ca$_v$2.1[EFa] and Ca$_v$2.1[EFb] isoforms play unique roles in shaping presynaptic plasticity: Ca$_v$2.1[EFa] is more effective in supporting neurotransmitter release and promotes PPD, while Ca$_v$2.1[EFb] displays a lower synaptic efficacy that favors PPF (Figures 7F and S7). Our findings are in line with a large body of evidence supporting the following model: at high-P$_r$ synapses displaying PPD, VGCCs are tightly localized at the presynaptic AZ, where they increase Ca$^{2+}$ locally, thus driving vesicle release effectively in response to a single AP; in contrast, at low-P$_r$ synapses with a prominent PPF, VGCCs are farther away from the AZ, thus boosting the residual Ca$^{2+}$ that facilitates release during repetitive stimulations but contributing little to the Ca$^{2+}$ signal at the AZ in response to single APs (Eggermann et al., 2012; Hoppa et al., 2012; Kaeser et al., 2011; Mochida et al., 1996; Vyleta and Jonas, 2014; Wu et al., 1999).
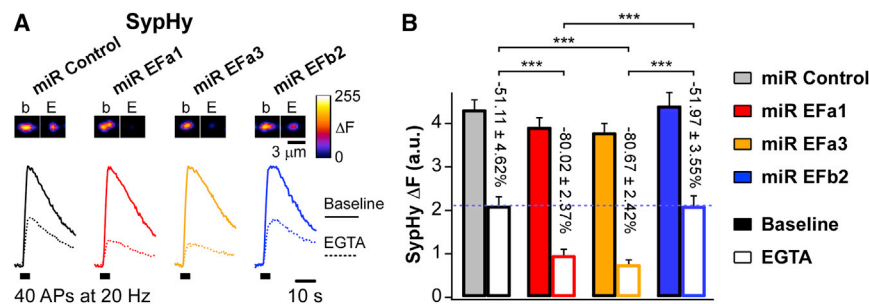
Figure 5. Knockdown of Ca$_v$2.1[EFa] Selectively Increases the Sensitivity of Vesicle Release to EGTA

(A) SypHy responses for miR control, miR EFa1, miR EFa3, and miR EFb2 to 40 APs at 20 Hz before (continuous line) and after (dotted line) EGTA-AM application (200 μM; loaded for 90 s, followed by 10 min wash). Traces are normalized to pre-EGTA responses in miR control. Inset: individual boutons for the four conditions (b, pre-EGTA; E, post-EGTA).
(B) Summary of experiments as in (A) (n = 10, 13, 12, and 11 independent experiments for miR control, miR EFa1, miR EFa3, and miR EFb2, respectively; ***p < 0.001). Sensitivity to EGTA is selectively increased by knockdown of Ca$_v$2.1[EFa].
Data are presented as mean ± SEM. See also Figure S4.

In our overexpression experiments, we used Ca$_v$2.1 channels devoid of the long C-terminal exon 47 (Figure 1B) because we wanted to investigate the functional consequences of alternative splicing at exon 37a/b while trying to minimize the interference by other domains. Inclusion of the C-terminal exon 47 generates Ca$_v$2.1 channels with additional 244 amino acids that carry motifs for binding to the PDZ domains of Mint1 and RIM proteins (Kaeser et al., 2011; Maximov et al., 1999) and to the SH3 domains of RIM-binding proteins (Davydova et al., 2014; Hibino et al., 2002). Although these interactions are important to target P/Q- and N-type Ca$^{2+}$ channels to vesicle release sites, P/Q-type channels devoid of exon 47 are abundant in the brain (Soong et al., 2002) and can accumulate efficiently at synapses, as previously documented (Cao and Tsien, 2010; Hu et al., 2005; Schneider et al., 2015) and as we report here (Figures S1–S3).

Additional interacting domains, such as those in the intracellular loop between domains II and III of Ca$_v$2.1 and Ca$_v$2.2 channels, which bind to SNARE proteins (Mochida et al., 1996; Rettig et al., 1996; Sheng et al., 1994), and those in the intracellular loop between domains I and II of VGCCs, which bind to auxiliary β subunits (Kiyonaka et al., 2007; Pragnell et al., 1994), play a key role in anchoring VGCCs at presynaptic sites. Specifically, auxiliary β subunits form a bridge between VGCC α$_1$ subunits and the AZ protein RIM1 (Kiyonaka et al., 2007), thus effectively linking VGCCs to the presynaptic cytomatrix. Indeed, we find that the auxiliary subunit β4 is required for efficient targeting of exogenous Ca$_v$2.1[EFa] and Ca$_v$2.1[EFb] to axons (Figure S1).

The differences in synaptic efficacy between Ca$_v$2.1[EFa] and Ca$_v$2.1[EFb] (Figures 1, 2, 6, S5, and S6) are likely due to a differential organization of the two splice isoforms at presynaptic sites, as we find marked differences in their presynaptic localization (Figures 4 and S1) and in their sensitivity to the slow Ca$^{2+}$ chelator EGTA (Figures 3 and 5). The EF-hand-like domains encoded by exons 37a and 37b might represent additional interacting domains important for the precise and differential positioning of P/Q-type channel isoforms relative to the neurotransmitter release machinery.

Although our experiments suggest that the primary difference between Ca$_v$2.1[EFa] and Ca$_v$2.1[EFb] lies in their spatial relationship to fuse-competent vesicles, we cannot rule out that differences in their biophysical properties might also contribute to setting synaptic efficacy at central synapses. The Ca$_v$2.1[EFb]-

dependent facilitation of synaptic transmission (Figures 1 and 6), however, could not be predicted by experiments in heterologous expression systems, where Ca$_v$2.1[EFb] shows little or no Ca$^{2+}$-dependent facilitation of the channel (Chaudhuri et al., 2004). Differences in the availability of Ca$^{2+}$-binding proteins regulating Ca$^{2+}$-dependent facilitation might however result in VGCCs with divergent functional properties between presynaptic boutons and heterologous expression systems (Lautermilch et al., 2005; Lee et al., 2002).

Alternative splicing at exons 37a and 37b is conserved across P/Q-, N-, and R-type Ca$^{2+}$ channels (Figure 1B; Gray et al., 2007), suggesting that it might represent a common mechanism to regulate the synaptic function of these VGCCs. Regarding N-type Ca$^{2+}$ channels, the Ca$_v$2.2[EFa] isoform is selectively expressed in capsaicin-responsive nociceptors of dorsal root ganglia (Bell et al., 2004), where it mediates thermal nociception (Altier et al., 2007; Andrade et al., 2010). In contrast, Ca$_v$2.2[EFb] is the isoform abundant throughout the nervous system (Bell et al., 2004).

Considering that the expression of Ca$_v$2.1[EFa] and Ca$_v$2.1[EFb] splice isoforms varies during development (Vigues et al., 2002), across brain regions (Bourinet et al., 1999; Chaudhuri et al., 2004), and in response to changes in neuronal network activity (Figures 7A–7C), their differential efficacy to promote synaptic transmission (Figures 2 and S6) likely contributes to the intersynaptic variability in P$_r$ and short-term synaptic plasticity. For instance, the increase in Ca$_v$2.1[EFa] expression that occurs during development (Vigues et al., 2002) correlates with the tightening of the coupling between VGCCs and Ca$^{2+}$ sensor observed during synapse maturation (Eggermann et al., 2012). Conversely, Ca$_v$2.1[EFb] predominates in neurons forming highly facilitating synapses, such as hippocampal granule cells (Vigues et al., 2002).

We found that the relative abundance of the two splice isoforms at the synapse is regulated in a homeostatic fashion to adapt presynaptic strength to changes in neuronal network activity (Figures 7 and S7). Specifically, hippocampal neurons selectively increase the expression of Ca$_v$2.1[EFa] in response to activity deprivation. Because this splice isoform drives the higher synaptic efficacy of the two, it can effectively support homeostatic upregulation of presynaptic release. This finding provides therefore a clear molecular basis for the previous
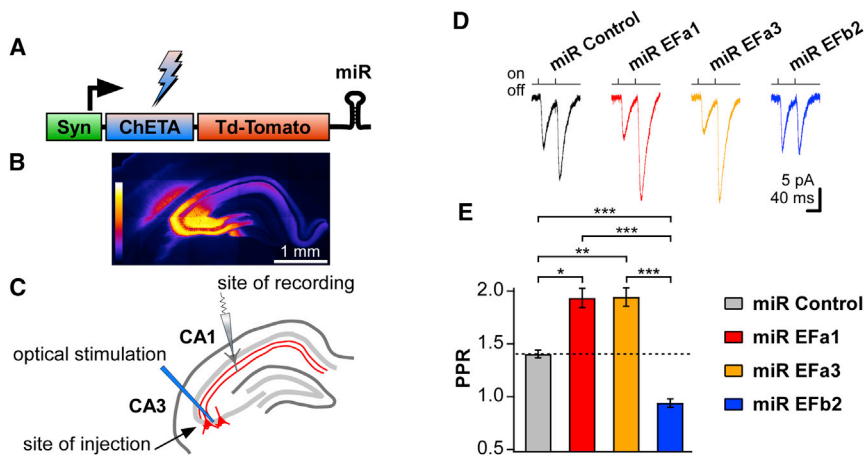
**Figure 6. Assessing the role of Ca$_v$2.1[EFa] and Ca$_v$2.1[EFb] in the Native Hippocampus by Targeted Stimulation of Knocked-Down Neurons with Optogenetics**

(A) Scheme of AAV constructs used for in vivo infection, containing a synapsin promoter (Syn), the ultrafast channelrhodopsin ChETA fused to TdTomato and, in the 3'UTR, Ca$_v$2.1 splice isoform-specific miRs.

(B) Hippocampal section showing that TdTomato fluorescence is limited to the CA3 region and its projections.

(C) Experimental configuration: laser beam was directed onto CA3 somata, and patch-clamp recordings were performed from CA1 pyramidal neurons.

(D) Two-millisecond-long blue light pulses shone at 20 Hz evoke EPSCs whose PPF is increased by miRs targeting Ca$_v$2.1[EFa] and abolished by miR for Ca$_v$2.1[EFb].

(E) Summary of PPRs for experiments as in (D) showing an increase in PPF for miR EFa1 and miR EFa3 and a decrease for miR EFb2, relative to miR control (n = 11, 9, 9, and 10 recordings for miR control, miR EFa1, miR EFa3, and miR EFb2, respectively; *p = 0.02, **p = 0.01, and ***p < 0.0004). Data are presented as mean ± SEM. See also Figures S4 and S5.

observations implicating VGCC-mediated Ca$^{2+}$ signals and their upregulation in presynaptic homeostatic plasticity (Frank et al., 2006; Jakawich et al., 2010; Lazarevic et al., 2011; Zhao et al., 2011) and highlights the importance of alternative splicing of P/Q-type Ca$^{2+}$ channels in shaping presynaptic function in an activity-dependent manner.

In summary, previous studies have described that different VGCC types are differentially recruited to the AZ, with P/Q-type channels generally being more effective than N- and R-type channels in eliciting neurotransmitter release (Wu et al., 1999), and that auxiliary subunits can effectively control the trafficking and gating of VGCCs. In particular, auxiliary $\alpha_2\delta$ subunits affect the coupling between synaptic VGCCs and the RRP at hippocampal synapses (Hoppa et al., 2012, but see Schneider et al., 2015). Our findings show that also the balance between two mutually exclusive splice variants of a pore-forming VGCC $\alpha_1$ subunit shapes synaptic transmission and plasticity. Importantly, hippocampal neurons regulate the relative abundance of the two splice isoforms in an activity-dependent manner. Considering that alternative splicing of $\alpha_1$ subunits is prominent in the brain (Lipscombe et al., 2013; Simms and Zamponi, 2014; Soong et al., 2002), it is tempting to speculate that a combinatorial splicing code might exist to match the expression of multiple VGCC splice isoforms to the specific needs of synaptic transmission under different activity states.

## EXPERIMENTAL PROCEDURES

### RNAi

Splice isoform-specific miRs for rat Ca$_v$2.1[EFa] (miR EFa1: TCCTTATAGT GAATGCGGCCG; miR EFa3: TTGCAAGCAACCCTATGAGGA) and Ca$_v$2.1 [EFb] (miR EFb2: ATCTGATACATGTCCGGGTAA) were generated using the BLOCK-iT kit (Invitrogen) and validated by western blotting and RT-qPCR. As a negative control (miR control), we used the pcDNA6.2-GW/EmGFP-miR-neg plasmid from the kit containing a sequence that does not target any known vertebrate gene. Detailed methods are described in the Supplemental Information.

### In Vivo Knockdown

AAV1/2 expressing the ultrafast channelrhodopsin ChETA, TdTomato, and Ca$_v$2.1 splice isoform-specific miRs were injected into the CA3 region of P18 rats, with coordinates of (A-P/M-L/D-V from Bregma) $-2.6/ \pm 2.9/-2.9$, as detailed in Supplemental Experimental Procedures.

### Electrophysiology in Primary Cultures

Whole-cell recordings were performed from pyramidal neurons of rat hippocampal cultures, continuously perfused with aCSF containing 140 mM NaCl, 2.5 mM KCl, 2.2 mM CaCl$_2$, 2.3 mM MgCl$_2$, 10 mM D-glucose, and 10 mM HEPES-NaOH (pH 7.38, osmolarity adjusted to 290 mOsm). A GABA$_A$ receptor blocker (100 μM picrotoxin) was routinely included in the aCSF. For EGTA-AM experiments, CaCl$_2$ was raised to 2.5 mM and MgCl$_2$ lowered to 1.5 mM. To isolate NMDAR-mediated EPSCs, CaCl$_2$ and MgCl$_2$ were lowered to 1.5 and 0.1 mM, respectively, and aCSF was supplemented with an NMDAR co-agonist (20 μM glycine) and an AMPAR blocker (2 μM NBQX). The intracellular solution contained 100 mM K-gluconate, 5 mM K-glutamate, 17 mM KCl, 5 mM NaCl, 0.5 mM EGTA, 5 mM MgCl$_2$, 4 mM K$_2$-ATP, 0.5 mM Na$_3$-GTP, 20 mM K$_2$-creatine phosphate, and 10 mM HEPES-KOH (pH 7.28, osmolarity adjusted to 280 mOsm). Pre- and postsynaptic neurons were voltage-clamped at $-70$ and $-50$ mV for AMPAR- and NMDAR-mediated EPSC recordings, respectively; in order to evoke synaptic transmission, unclamped Na$^+$ spikes were elicited in the presynaptic neuron by delivering one or two depolarizing stimuli (+30 mV, 2 ms long) at various interstimulus intervals (see Supplemental Experimental Procedures).

### Electrophysiology and Optogenetics in Acute Brain Slices

All experiments were carried out in accordance with the guidelines established by the European Communities Council (Directive 2010/63/EU of March 4, 2014), and were approved by the Italian Ministry of Health. Fifteen to 24 days post-injection, sagittal slices of the rat hippocampus (350 μm thick) were prepared with a Vibratome (Leica VT1200S). Slices were maintained submerged in gassed (95% O$_2$, 5% CO$_2$) aCSF containing 123 mM NaCl, 1.25 mM KCl, 1.25 mM KH$_2$PO4, 1.5 mM MgCl$_2$, 1 mM CaCl$_2$, 25 mM NaHCO$_3$, 2 mM NaPyruvate, and 18 mM glucose (osmolarity adjusted to 300 mOsm). After recovering for 30 min at 37°C and for $\geq$30 min at room temperature, slices were transferred to a submerged recording chamber and superfused with the same aCSF used for recovery supplemented with 1.5 mM CaCl$_2$ (total Ca$^{2+}$ 2.5 mM). Whole-cell recordings were obtained from pyramidal neurons in the proximal to medial tract of the CA1 region. The intracellular solution contained 110 mM K-gluconate, 22 mM KCl, 5 mM NaCl, 0.5 mM EGTA, 3 mM MgCl$_2$, 4 mM Mg-ATP, 0.5 mM Na$_3$-GTP, 20 mM K$_2$-creatine phosphate,
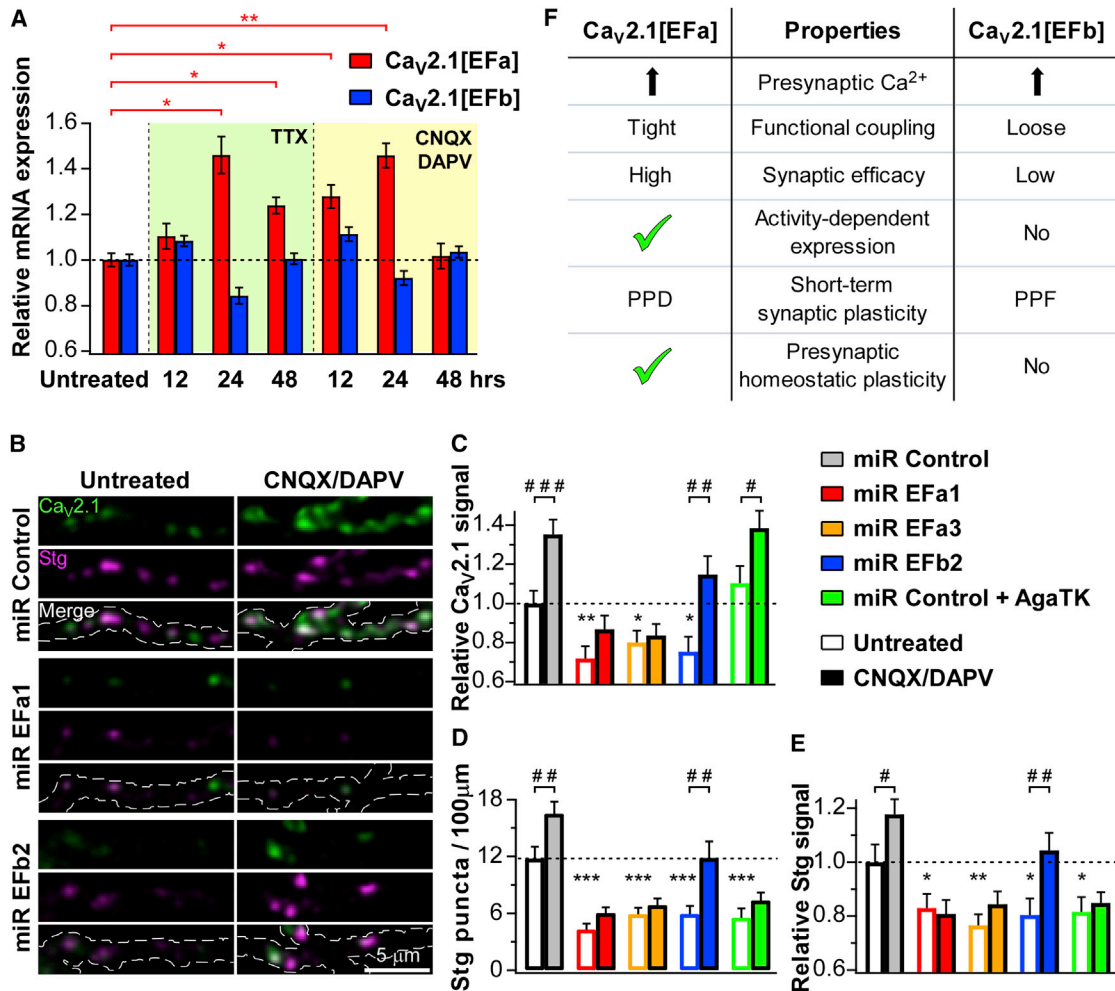
**Figure 7. Expression of Ca$_v$2.1[EFa] Is Selectively Regulated by Activity, and It Is Required for Presynaptic Homeostatic Plasticity**

(A) Network activity of primary hippocampal cultures was suppressed with either TTX (1 μM) or CNQX (20 μM) and D-APV (100 μM) for the indicated time period. RT-qPCR analysis was performed on RNA isolated at 18 DIV (n = 6 independent experiments). Data are normalized to untreated controls. Chronic activity deprivation with either TTX or CNQX/DAPV increases selectively the mRNA of Ca$_v$2.1[EFa], with the effect being maximal after 24 hr (*p $\leq$ 0.04, **p = 0.004).

(B–E) Effects of Ca$_v$2.1 splice isoform-specific knockdown on synaptotagmin antibody uptake in untreated and silenced cultures. (B) Confocal microscopy images of primary hippocampal axons expressing the indicated microRNAs (miRs) under basal conditions (untreated) and upon activity deprivation with CNQX (20 μM) and D-APV (100 μM) for 24 hr (CNQX/DAPV). Ca$_v$2.1 (green) was detected with an antibody recognizing both splice isoforms; synaptotagmin antibody uptake (Stg, magenta) was carried out at 37°C for 12 min; transfected axons were identified with TdTomato (outline indicated by dashed lines in merge). (C–E) Quantification of experiments as in (B) showing that in untreated cultures (white-filled bars), knockdown of either Ca$_v$2.1[EFa] (miR EFa1 or miR EFa3) or Ca$_v$2.1 [EFb] (miR EFb2) reduces the total number of Stg puncta (D), their fluorescence intensity (E), and the fluorescent signal of Ca$_v$2.1 co-localizing with Stg (C), relative to controls (miR control). The number and intensity of Stg puncta is also reduced by pharmacological blockade of Ca$_v$2.1 with ω-agatoxin TK (300 nM; miR control+AgaTK; *p < 0.05, **p < 0.004, and ***p $\leq$ 0.0003). Chronic treatment with CNQX and D-APV (color-filled bars) increases Stg uptake and Ca$_v$2.1 signal in controls. Both effects are blocked by knockdown of Ca$_v$2.1[EFa] but not by knockdown of Ca$_v$2.1[EFb]. The up-scaling of Stg is also prevented by blocking pharmacologically Ca$_v$2.1 (miR control+AgaTK; n = 40, 40, 38, 36, and 37 fields of view for miR control, miR EFa1, miR EFa3, miR EFb2, and miR control+AgaTK untreated, respectively; n = 40, 38, 39, 38, and 39 fields of view for miR EFa1, miR EFa3, miR EFb2, and miR control+AgaTK CNQX/DAPV, respectively; #p < 0.05, ##p < 0.01, and ###p = 0.0008). These data suggest that the increase in Ca$_v$2.1 at synapses upon activity deprivation is due largely to Ca$_v$2.1[EFa] and that this splice isoform is selectively required for the expression of presynaptic homeostatic plasticity. Data are presented as mean ± SEM.

(F) Summary of the differential properties of Ca$_v$2.1 splice isoforms on synaptic transmission and presynaptic plasticity.

See also Figures S6 and S7.

10 mM HEPES-KOH (pH 7.28, osmolarity adjusted to 290 mOsm). Experiments were performed in the presence of 10 μM bicuculline. EPSCs were evoked with a 473 nm Blue Laser (MBL-III-473 Solid State 1–200 mW; Information Unlimited) coupled via a 20× 0.40 N.A. objective to an optical fiber (250 μm in diameter) positioned directly on CA3 somata. Stimulation strength (1–3 mW at fiber exit) was adjusted with neutral density filters to yield small, but clearly

detectable, EPSCs (<30 pA peak amplitude at −70 mV; see Supplemental Experimental Procedures).

**Live Imaging**
Imaging was performed in rat primary cultures using SyGCaMP3, SyGCaMP6s, or Fluo-4 as a reporter for Ca$^{2+}$ and SypHy as a reporter for vesicle turnover.

SypHy was imaged in aCSF containing 140 mM NaCl, 2.5 mM KCl, 2.2 mM CaCl$_2$, 1.5 mM MgCl$_2$, 13 mM D-glucose, 0.01 mM CNQX, 0.05 mM D-APV, and 12 mM HEPES-NaOH (pH 7.38, osmolarity adjusted to 320 mOsm). Images were captured at 2 Hz with 100 ms integration times using a cooled charge-coupled device (CCD) camera (ORCA-R2; Hamamatsu) and analyzed offline using ImageJ (http://imagej.nih.gov/ij) and the plugin Time Series Analyzer (http://imagej.nih.gov/ij/plugins/time-series.html) using regions of interest (ROIs) 3.2 μm in diameter. The intensity of a twin ROI positioned within 10 μm of the first was used to subtract the local background noise. Signals were quantified as $\Delta F = F - F_0$, where $F_0$ was measured over a 5 s period prior to stimulation (see Supplemental Experimental Procedures).

### Synaptotagmin Antibody Live Uptake

Cultures were treated with CNQX (20 μM) and D-APV (100 μM) 24 hr prior to experiments. N-type Ca$^{2+}$ channels were always blocked with ω-conotoxin GVIA (1 μM) starting 30 min prior to uptake. A subset of coverslips treated also with ω-agatoxin TK (300 nM) for the same time period served as negative control. Neurons were rinsed twice in aCSF containing 140 mM NaCl, 5 mM KCl, 2.2 mM CaCl$_2$, 1.5 mM MgCl$_2$, 15 mM D-glucose, 0.01 mM CNQX, 0.05 mM D-APV, 0.001 mM ω-conotoxin GVIA, and 12 mM HEPES-NaOH, with or without 0.0003 mM ω-agatoxin TK (pH 7.38, osmolarity adjusted to 320 mOsm), before performing the synaptotagmin antibody live uptake in the same aCSF for 12 min at 37°C with a mouse antibody against the luminal domain of synaptotagmin 1 (1:200; catalog no. 105311, Synaptic Systems). After three washes in the same aCSF, neurons were fixed and processed for immunofluorescence, as described in Supplemental Experimental Procedures.

### Statistics

Unless otherwise stated, statistical differences were assessed using paired and unpaired two-tailed Student's t test and the one-way ANOVA test followed by the Tukey-Kramer post-test, as required. Analysis of covariance was used for Figures 1E, 3D, and 6E and the Kruskal-Wallis test followed by Dunn's multiple comparison post-test for Figure 1G (Prism 5; GraphPad Software). Unless otherwise stated, average data are expressed as mean + SEM.

### SUPPLEMENTAL INFORMATION

Supplemental Information includes Supplemental Experimental Procedures and seven figures and can be found with this article online at http://dx.doi.org/10.1016/j.celrep.2017.06.055.

### REFERENCES

Altier, C., Dale, C.S., Kisilevsky, A.E., Chapman, K., Castiglioni, A.J., Matthews, E.A., Evans, R.M., Dickenson, A.H., Lipscombe, D., Vergnolle, N., and Zamponi, G.W. (2007). Differential role of N-type calcium channel splice isoforms in pain. J. Neurosci. 27, 6363–6373.

Andrade, A., Denome, S., Jiang, Y.Q., Marangoudakis, S., and Lipscombe, D. (2010). Opioid inhibition of N-type Ca$^{2+}$ channels and spinal analgesia couple to alternative splicing. Nat. Neurosci. 13, 1249–1256.

Bell, T.J., Thaler, C., Castiglioni, A.J., Helton, T.D., and Lipscombe, D. (2004). Cell-specific alternative splicing increases calcium channel current density in the pain pathway. Neuron 41, 127–138.

Bourinet, E., Soong, T.W., Sutton, K., Slaymaker, S., Mathews, E., Monteil, A., Zamponi, G.W., Nargeot, J., and Snutch, T.P. (1999). Splicing of alpha 1A subunit gene generates phenotypic variants of P- and Q-type calcium channels. Nat. Neurosci. 2, 407–415.

Cao, Y.Q., and Tsien, R.W. (2010). Different relationship of N- and P/Q-type Ca$^{2+}$ channels to channel-interacting slots in controlling neurotransmission at cultured hippocampal synapses. J. Neurosci. 30, 4536–4546.

Chaudhuri, D., Chang, S.Y., DeMaria, C.D., Alvania, R.S., Soong, T.W., and Yue, D.T. (2004). Alternative splicing as a molecular switch for Ca$^{2+}$/calmodulin-dependent facilitation of P/Q-type Ca$^{2+}$ channels. J. Neurosci. 24, 6334–6342.

Chavez-Noriega, L.E., and Stevens, C.F. (1994). Increased transmitter release at excitatory synapses produced by direct activation of adenylate cyclase in rat hippocampal slices. J. Neurosci. 14, 310–317.

Davydova, D., Marini, C., King, C., Klueva, J., Bischof, F., Romorini, S., Montenegro-Venegas, C., Heine, M., Schneider, R., Schröder, M.S., et al. (2014). Bassoon specifically controls presynaptic P/Q-type Ca(2+) channels via RIM-binding protein. Neuron 82, 181–194.

Dreosti, E., Odermatt, B., Dorostkar, M.M., and Lagnado, L. (2009). A genetically encoded reporter of synaptic activity in vivo. Nat. Methods 6, 883–889.

Eggermann, E., Bucurenciu, I., Goswami, S.P., and Jonas, P. (2012). Nanodomain coupling between Ca$^{2+}$ channels and sensors of exocytosis at fast mammalian synapses. Nat. Rev. Neurosci. 13, 7–21.

Frank, C.A., Kennedy, M.J., Goold, C.P., Marek, K.W., and Davis, G.W. (2006). Mechanisms underlying the rapid induction and sustained expression of synaptic homeostasis. Neuron 52, 663–677.

Graves, T.D., Imbrici, P., Kors, E.E., Terwindt, G.M., Eunson, L.H., Frants, R.R., Haan, J., Ferrari, M.D., Goadsby, P.J., Hanna, M.G., et al. (2008). Premature stop codons in a facilitating EF-hand splice variant of CaV2.1 cause episodic ataxia type 2. Neurobiol. Dis. 32, 10–15.

Gray, A.C., Raingo, J., and Lipscombe, D. (2007). Neuronal calcium channels: splicing for optimal performance. Cell Calcium 42, 409–417.

Gunaydin, L.A., Yizhar, O., Berndt, A., Sohal, V.S., Deisseroth, K., and Hegemann, P. (2010). Ultrafast optogenetic control. Nat. Neurosci. 13, 387–392.

Hessler, N.A., Shirke, A.M., and Malinow, R. (1993). The probability of transmitter release at a mammalian central synapse. Nature 366, 569–572.

Hibino, H., Pironkova, R., Onwumere, O., Vologodskaia, M., Hudspeth, A.J., and Lesage, F. (2002). RIM binding proteins (RBPs) couple Rab3-interacting molecules (RIMs) to voltage-gated Ca(2+) channels. Neuron 34, 411–423.

Hoppa, M.B., Lana, B., Margas, W., Dolphin, A.C., and Ryan, T.A. (2012). α2δ expression sets presynaptic calcium channel abundance and release probability. Nature 486, 122–125.

Hu, Q., Saegusa, H., Hayashi, Y., and Tanabe, T. (2005). The carboxy-terminal tail region of human Cav2.1 (P/Q-type) channel is not an essential determinant for its subcellular localization in cultured neurones. Genes Cells 10, 87–96.

Jakawich, S.K., Nasser, H.B., Strong, M.J., McCartney, A.J., Perez, A.S., Rakesh, N., Carruthers, C.J., and Sutton, M.A. (2010). Local presynaptic activity gates homeostatic changes in presynaptic function driven by dendritic BDNF synthesis. Neuron 68, 1143–1158.

Kaeser, P.S., Deng, L., Wang, Y., Dulubova, I., Liu, X., Rizo, J., and Südhof, T.C. (2011). RIM proteins tether Ca$^{2+}$ channels to presynaptic active zones via a direct PDZ-domain interaction. Cell 144, 282–295.

Kiyonaka, S., Wakamori, M., Miki, T., Uriu, Y., Nonaka, M., Bito, H., Beedle, A.M., Mori, E., Hara, Y., De Waard, M., et al. (2007). RIM1 confers sustained activity and neurotransmitter vesicle anchoring to presynaptic Ca$^{2+}$ channels. Nat. Neurosci. 10, 691–701.

Lautermilch, N.J., Few, A.P., Scheuer, T., and Catterall, W.A. (2005). Modulation of CaV2.1 channels by the neuronal calcium-binding protein visinin-like protein-2. J. Neurosci. 25, 7062–7070.

Lazarevic, V., Schöne, C., Heine, M., Gundelfinger, E.D., and Fejtova, A. (2011). Extensive remodeling of the presynaptic cytomatrix upon homeostatic adaptation to network activity silencing. J. Neurosci. 31, 10189–10200.

Lee, A., Westenbroek, R.E., Haeseleer, F., Palczewski, K., Scheuer, T., and Catterall, W.A. (2002). Differential modulation of Ca(v)2.1 channels by calmodulin and $Ca^{2+}$-binding protein 1. Nat. Neurosci. 5, 210–217.

Lipscombe, D., Allen, S.E., and Toro, C.P. (2013). Control of neuronal voltage-gated calcium ion channels from RNA to protein. Trends Neurosci. 36, 598–609.

Mantuano, E., Romano, S., Veneziano, L., Gellera, C., Castellotti, B., Caimi, S., Testa, D., Estienne, M., Zorzi, G., Bugiani, M., et al. (2010). Identification of novel and recurrent CACNA1A gene mutations in fifteen patients with episodic ataxia type 2. J. Neurol. Sci. 291, 30–36.

Maximov, A., Südhof, T.C., and Bezprozvanny, I. (1999). Association of neuronal calcium channels with modular adaptor proteins. J. Biol. Chem. 274, 24453–24456.

Mochida, S., Sheng, Z.H., Baker, C., Kobayashi, H., and Catterall, W.A. (1996). Inhibition of neurotransmission by peptides containing the synaptic protein interaction site of N-type $Ca^{2+}$ channels. Neuron 17, 781–788.

Pragnell, M., De Waard, M., Mori, Y., Tanabe, T., Snutch, T.P., and Campbell, K.P. (1994). Calcium channel beta-subunit binds to a conserved motif in the I-II cytoplasmic linker of the alpha 1-subunit. Nature 368, 67–70.

Raj, B., and Blencowe, B.J. (2015). Alternative splicing in the mammalian nervous system: recent insights into mechanisms and functional roles. Neuron 87, 14–27.

Reid, C.A., Bekkers, J.M., and Clements, J.D. (1998). N- and P/Q-type $Ca^{2+}$ channels mediate transmitter release with a similar cooperativity at rat hippocampal autapses. J. Neurosci. 18, 2849–2855.

Rettig, J., Sheng, Z.H., Kim, D.K., Hodson, C.D., Snutch, T.P., and Catterall, W.A. (1996). Isoform-specific interaction of the alpha1A subunits of brain $Ca^{2+}$ channels with the presynaptic proteins syntaxin and SNAP-25. Proc. Natl. Acad. Sci. U S A 93, 7363–7368.

Rosenmund, C., Clements, J.D., and Westbrook, G.L. (1993). Nonuniform probability of glutamate release at a hippocampal synapse. Science 262, 754–757.

Schneider, R., Hosy, E., Kohl, J., Klueva, J., Choquet, D., Thomas, U., Voigt, A., and Heine, M. (2015). Mobility of calcium channels in the presynaptic membrane. Neuron 86, 672–679.

Scholz, K.P., and Miller, R.J. (1995). Developmental changes in presynaptic calcium channels coupled to glutamate release in cultured rat hippocampal neurons. J. Neurosci. 15, 4612–4617.

Sheng, Z.H., Rettig, J., Takahashi, M., and Catterall, W.A. (1994). Identification of a syntaxin-binding site on N-type calcium channels. Neuron 13, 1303–1313.

Simms, B.A., and Zamponi, G.W. (2014). Neuronal voltage-gated calcium channels: structure, function, and dysfunction. Neuron 82, 24–45.

Soong, T.W., DeMaria, C.D., Alvania, R.S., Zweifel, L.S., Liang, M.C., Mittman, S., Agnew, W.S., and Yue, D.T. (2002). Systematic identification of splice variants in human P/Q-type channel alpha1(2.1) subunits: implications for current density and $Ca^{2+}$-dependent inactivation. J. Neurosci. 22, 10142–10152.

Vigues, S., Gastaldi, M., Massacrier, A., Cau, P., and Valmier, J. (2002). The alpha(1A) subunits of rat brain calcium channels are developmentally regulated by alternative RNA splicing. Neuroscience 113, 509–517.

Vyleta, N.P., and Jonas, P. (2014). Loose coupling between $Ca^{2+}$ channels and release sensors at a plastic hippocampal synapse. Science 343, 665–670.

Wu, L.G., Westenbroek, R.E., Borst, J.G., Catterall, W.A., and Sakmann, B. (1999). Calcium channel types with distinct presynaptic localization couple differentially to transmitter release in single calyx-type synapses. J. Neurosci. 19, 726–736.

Zhao, C., Dreosti, E., and Lagnado, L. (2011). Homeostatic synaptic plasticity through changes in presynaptic calcium influx. J. Neurosci. 31, 7492–7496.